Res Chem Intermed (2015) 41:9673–9685
DOI 10.1007/s11164-015-1956-y

A new optical sensor for Al^{3+}/Fe^{3+} based on PET and chelation-enhanced fluorescence

Meiling Gao[1] · Puhui Xie[2] · Lingyu Wang[1] · Xiaohui Miao[1] · Fengqi Guo[1]

Received: 25 November 2014 / Accepted: 5 February 2015 / Published online: 10 March 2015

Abstract A simple probe (compound **1**) sensing Al^{3+} or Fe^{3+} by suppression of photoinduced electron/energy transfer (PET) process and chelation-enhanced fluorescence is described. Compound **1** was prepared from 2-(bromomethyl)benzo[*d*]thiazole and pyridine-2,6-diamine. Compound **1** showed a much stronger fluorescence response to Al(III) than to Fe(III). The best fluorescence response of **1** to Al^{3+} was found to be at pH near 7. The results indicated that **1** could be a promising fluorescent turn-on chemosensor for Al^{3+} or Fe^{3+}. Ratiometric sensing of **1** to Al^{3+} or Fe^{3+} was accomplished by plotting the absorbance ratio at 338 to 310 nm versus Al^{3+} or Fe^{3+} concentration. The fluorescent turn-on response of **1** to Al^{3+} or Fe^{3+} can be attributed to suppression of PET process and chelation-enhanced fluorescence upon binding with Al^{3+} or Fe^{3+}. The binding mode of **1**-Al^{3+} or **1**-Fe^{3+} was found to be a 1:1 complex based on Job's plot, electrospray ionization (ESI) mass spectroscopy (MS) data, and density functional theory (DFT) calculation results.

Keywords Fluorescent probe · Ratiometric · PET · Chelation-enhanced fluorescence · Al(III)

Electronic supplementary material The online version of this article (doi:10.1007/s11164-015-1956-y) contains supplementary material, which is available to authorized users.

✉ Puhui Xie
phxie2013@163.com

✉ Fengqi Guo
fqguo@zzu.edu.cn

[1] College of Chemistry and Molecular Engineering, Zhengzhou University, Zhengzhou 450001, People's Republic of China

[2] College of Sciences, Henan Agricultural University, Zhengzhou 450002, People's Republic of China

Introduction

Aluminum, the third most abundant element after oxygen and silicon in the Earth's crust [1], is distributed ubiquitously in our daily life. Aluminum-containing derivatives are widely used in food additives, water treatment, and medicine [2]. However, overloading with aluminum will lead to malfunction of the human central nervous system [3]. Ferric ion is the most familiar metal ion, being found as an essential element in myoglobin, hemoglobin, and cytochromes, and playing an indispensable role in many biological processes such as cellular metabolism, gene regulation, electron transfer, and regulation of cell growth and differentiation [4–6]. Nonetheless, high concentration of ferric ion in organisms or the environment can induce biological disorders such as anemia, liver and kidney damage, heart failure, and diabetes, and cause serious environmental pollution [7, 8]. Therefore, it is important to develop efficient methods for detection and quantification of Al^{3+} or Fe^{3+} for food safety and quality control, clinical, and environmental applications. Among the various methods, fluorescence spectroscopy has become a powerful tool for sensing trace amounts of samples because of its simplicity, sensitivity, and fast response time [9–14]. Therefore, it is crucial to develop suitable fluorescent probes for Al^{3+} or Fe^{3+}.

Many kinds of signaling mechanisms have been proposed and applied in fluorescent detection of Al^{3+} or Fe^{3+}, including photoinduced electron/energy transfer (PET) [15–19], intramolecular charge transfer (ICT) [20–22], fluorescence resonance energy transfer (FRET) [23–25], excited-state intramolecular proton transfer [26], spirolactam to ring-open equilibrium of rhodamine derivatives [27–29], chelation-enhanced fluorescence [30–32], inhibiting nonradiative process by complexation of metal cations to C=N group [19, 32], etc. It is generally recognized that one probe with a fluorescent turn-on signal for specific species is more efficient [33, 34] than one with fluorescent quenching due to high signal-to-noise ratio. As the paramagnetic nature of Fe^{3+} always leads to a quenching ability, fluorescence enhancement through chelation of Fe^{3+} with a probe is a challenging research topic in vitro as well as in vivo. Although several "turn-on" probes that work with selective response to Al^{3+} or Fe^{3+} have been reported [35–38], their poor solubility in aqueous solution and complicated synthetic processes inhibit practical applications. New fluorescent sensors with simple synthetic processes and improved solubility in water have been developed in our group [39, 40]. In this work, a simple probe for Al^{3+} or Fe^{3+} with fluorescent enhancement was designed and synthesized. The nitrogen and sulfur atoms in **1** are well-known acceptor sites for metal ions. If probe **1** is coordinated with a certain metal ion, its molecular skeleton will be fixed with rigidity. Chelation of Al^{3+} or Fe^{3+} with probe **1** will result in fluorescent enhancement and shifts in absorption bands.

Experimental

All chemicals of analytical grade for syntheses were purchased from commercial suppliers and used without further purification. Tetrahydrofuran (THF) of spectroscopic grade and deionized water were used throughout the spectroscopic experiments as solvents. Nuclear magnetic resonance (NMR) spectra were recorded with a 300-MHz Varian spectrometer. Electrospray ionization mass spectra (ESI–MS) were measured on an LC-MSD-Trap-SL instrument. Fluorescence spectra were measured with a Cary Eclipse fluorescence spectrometer. UV–Vis absorption spectra were obtained on a UV-5200PC UV/vis spectrophotometer.

Stock solution of **1** (30 μM) in THF/H_2O (9/1, v/v) was prepared for spectroscopic investigations. Stock solutions of metal ions (1 mM) were prepared in deionized water from nitrates or chlorides of Na^+ (alkaline metal ion), Mg^{2+}, Ca^{2+} (alkaline earth metal ions), Al^{3+} (group IIIA metal ion), Mn^{2+}, Fe^{3+}, Co^{2+}, Ni^{2+}, Cu^{2+}, Zn^{2+} (first-row transition-metal ions), and Cd^{2+}, Hg^{2+}, Pb^{2+} (toxic heavy-metal ions) of analytical grade. In titration experiments, 3 mL stock solution of **1** was put into a quartz optical cell with optical path of 1 cm. Stock solution of each metal ion was added into the quartz optical cell step by step via a microsyringe, and the solution was stirred for 5 min before recording spectra. For fluorescence measurements, the excitation wavelength was provided at 310 nm, and emission was collected from 320 to 550 nm. The excitation slit and emission slit were both set at 5 nm.

The synthetic process of **1** is shown in Scheme 1. The intermediate **2** was synthesized according to literature [41].

Synthesis of 1

To a mixture of 2,6-diaminopyridine (109 mg, 1 mmol) and anhydrous K_2CO_3 (303 mg, 2.2 mmol) in CH_3CN (15 mL), a solution of 2-(bromomethyl)benzothiazole **2** (510 mg, 2.23 mmol) in 15 mL THF/CH_3CN (4/1, v/v) was added dropwise within 20 min. The mixture was stirred at room temperature for 72 h. Then, the solvents were removed under reduced pressure. The residue was dissolved in dichloromethane (40 mL) and washed three times with water. The organic phase was dried over anhydrous sodium sulfate. After removing the solvents, the crude product was subjected to column chromatography on silica gel with petroleum ether/ethyl acetate (1/1, v/v) to afford an off-white solid (110 mg, 43.2 %). ^{1}H NMR ($CDCl_3$) δ (ppm): 4.24 (s, 2H), 4.90 (*d*, J = 6.0 Hz, 2H), 5.16 (*t*, J = 6.0 Hz, 1H),

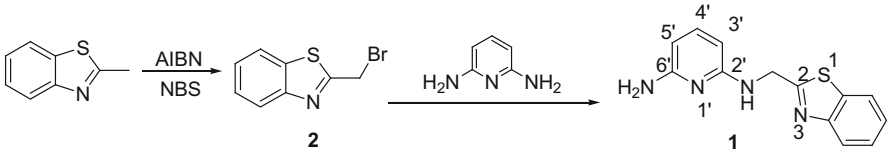

Scheme 1 Synthetic process of **1**

5.85–5.90 (m, 2H), 7.19–7.25 (m, 1H), 7.31–7.37 (m, 1H), 7.42–7.48 (m, 1H), 7.83 (*t*, $J = 8.0$ Hz, 1H), 7.96 (*d*, $J = 8.0$ Hz, 1H) (Fig. S1, Electronic Supplementary Material, ESM). ^{13}C NMR ($CDCl_3$), δ (ppm): 44.76, 96.54, 97.90, 121.72, 122.67, 124.83, 125.91, 135.14, 139.55, 153.29, 157.00, 157.54, 172.70 (Fig. S2, ESM). MS (ESI–MS): *m/z* calculated for $C_{13}H_{12}N_4S$, 256.33 $[M]^+$. Found: 256.2, 257.2 $[M + H]^+$ (Fig. S3, ESM).

Results and discussion

The response of fluorescence spectra to Al^{3+} or Fe^{3+}

The response of **1** to various metal ions, such as Na^+ (alkaline metal ion), Mg^{2+}, Ca^{2+} (alkaline earth metal ions), Al^{3+} (group IIIA metal ion), Mn^{2+}, Fe^{3+}, Co^{2+}, Ni^{2+}, Cu^{2+}, Zn^{2+} (first-row transition-metal ions), and Cd^{2+}, Hg^{2+}, Pb^{2+} (toxic heavy-metal ions) was investigated firstly by fluorescence spectra (Fig. 1). It could be seen that **1** (30 μmol/L) exhibited no fluorescence in THF/H_2O (9/1, v/v) solution. The intramolecular photoinduced electron transfer (PET) effect from the lone pair of electrons of the N atom on –NH– of pyridine group to the adjacent benzo[*d*]thiazole would result in no fluorescence of **1**. However, addition of Al^{3+} (30 μmol/L) caused an outstanding fluorescence enhancement centered at 393 nm. Addition of Fe^{3+} (30 μmol/L) caused a moderate fluorescence enhancement centered at 393 nm. Addition of Cu^{2+} (30 μmol/L) increased the fluorescence intensity of **1** very slightly. The fluorescence intensity of **1** at 393 nm was not increased after addition of 30 μmol/L Na^+, Ca^{2+}, Mg^{2+}, Co^{2+}, Mn^{2+}, Zn^{2+}, Cd^{2+}, Ni^{2+}, Pb^{2+} or Hg^{2+}, respectively. This result indicates that compound **1** shows superior selectivity towards Al^{3+} over Fe^{3+} and that compound **1** could be used as a turn-on fluorescence sensor for Al^{3+} or Fe^{3+}. The time dependence of the response of **1** to Al^{3+} or Fe^{3+} was investigated by recording the fluorescence intensity at 393 nm over time (Fig. S4, ESM). The results revealed that the reaction of compound **1** (30 μM) and Al^{3+} (100 μM) or Fe^{3+} (100 μM) was completed within

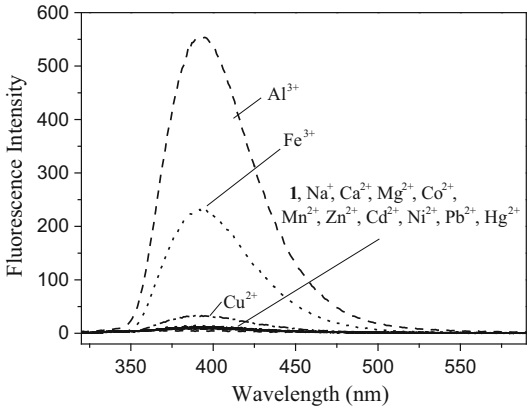

Fig. 1 Fluorescence spectra of **1** (30 μmol/L) in the presence of different metal ions (30 μmol/L) in THF/H_2O (9:1, v/v)

5 min. Therefore, all measurements were performed after mixing and stirring for 5 min.

The fluorescence spectra of **1** upon titration of Al^{3+} or Fe^{3+} are shown in Fig. 2a and b, respectively. A new emission band centered at 393 nm appeared, and the fluorescence was gradually enhanced upon gradual addition of Al^{3+} or Fe^{3+}. The maximum fluorescent enhancement (67-fold and 28-fold for Al^{3+} and Fe^{3+}, respectively) was observed at 393 nm when the amounts of metal ions and **1** were equal. The fluorescence intensity at 393 nm and the concentration of Al^{3+} or Fe^{3+} showed good linear relationship in the range from 2 to 40 μM (inset in Fig. 2a, b, respectively). The detection limit of **1** for Al^{3+} and Fe^{3+} was determined to be 29 and 46 nM (3σ/slope), respectively. The fluorescence enhancement for **1** in the presence of Al^{3+} or Fe^{3+} could be ascribed to the fixing in the molecular skeleton

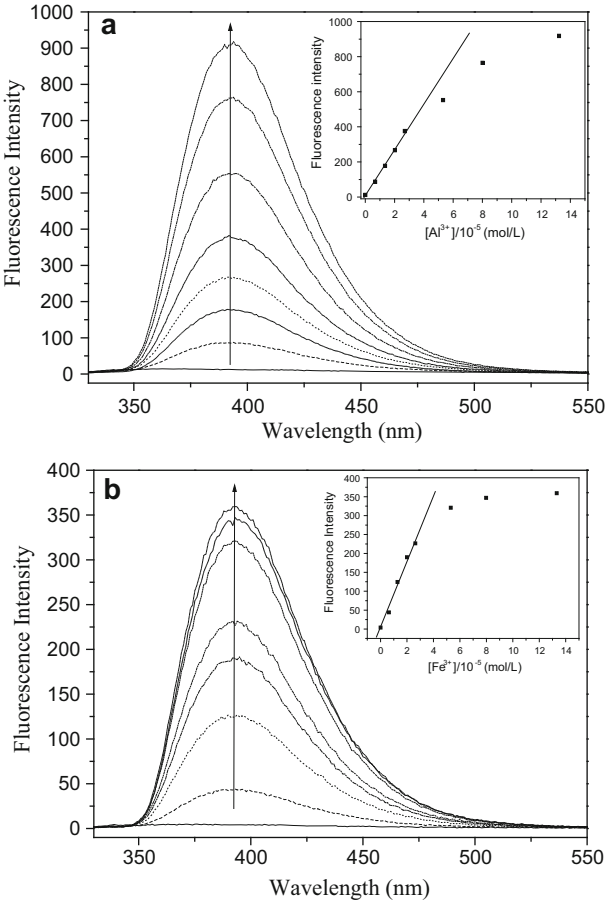

Fig. 2 **a** Fluorescence spectra of **1** (30 μmol/L) upon addition of Al^{3+} (*inset* fluorescence intensity at 393 nm of **1** as a function of Al^{3+} concentration). **b** Fluorescence spectra of **1** (30 μmol/L) upon addition of Fe^{3+} (*inset* fluorescence intensity at 393 nm of **1** as a function of Fe^{3+} concentration)

increasing the rigidity of **1** and decreasing the PET effect of the N atom on –NH– of pyridine group, after it was coordinated with Al^{3+} or Fe^{3+}.

Job's plots were used to determine the stoichiometries between **1** and Al^{3+} as well as **1** and Fe^{3+}. It can be seen in Fig. 3 that the fluorescent maxima of **1** are both at molar fraction of 0.5 for Al^{3+} or Fe^{3+}, indicating that the stoichiometries between **1** and Al^{3+} as well as **1** and Fe^{3+} are both 1:1.

As several kinds of metal ions often coexist in one system, coexisting metal ions may interfere with the detection of target ions. To determine the influence of other cations on the fluorescent detection of Al^{3+} or Fe^{3+} in THF/H_2O (9/1, v/v) solution, 300 μmol/L of metal ions such as Na^+, Hg^{2+}, Mg^{2+}, Mn^{2+}, Co^{2+}, Ca^{2+}, Cd^{2+}, Cu^{2+}, Pb^{2+}, Zn^{2+}, and Ni^{2+} were added to the solution of **1**-Al^{3+} or **1**-Fe^{3+}, respectively. As shown in Fig. 4a, b, the fluorescence intensity of **1**-Al^{3+} or **1**-Fe^{3+} was almost unaffected by the presence of the other metal ions. Although Cd^{2+} caused a slight decrease in the fluorescence intensity of **1**-Al^{3+} or **1**-Fe^{3+}, this was negligible compared with the enhancement of the fluorescence upon addition of Al^{3+} or Fe^{3+}. Based on these results, it was inferred that **1** could be a potential turn-on fluorescent probe for Al^{3+} or Fe^{3+} with high selectivity and high sensitivity in THF/H_2O (9/1, v/v) solution.

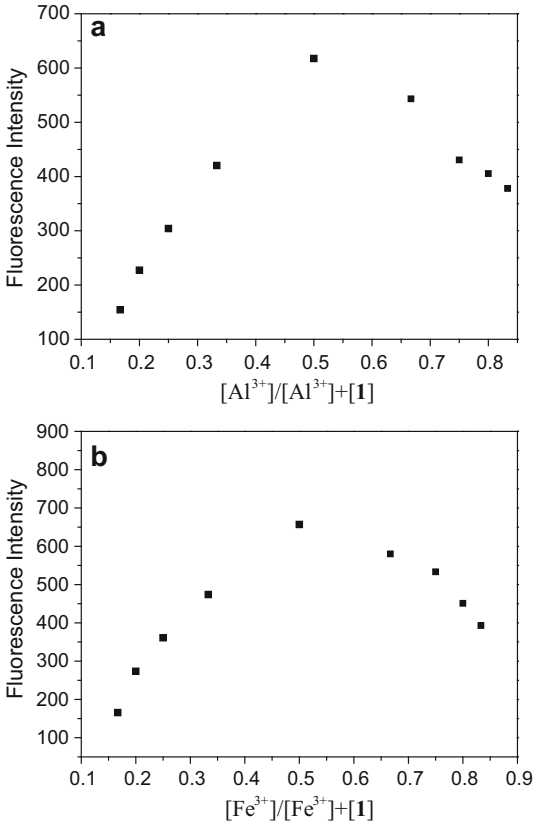

Fig. 3 Job's plot evaluated from the fluorescence spectra of **1** and Al^{3+} **a** or Fe^{3+} **b** at 393 nm in THF/H_2O (9:1, v/v)

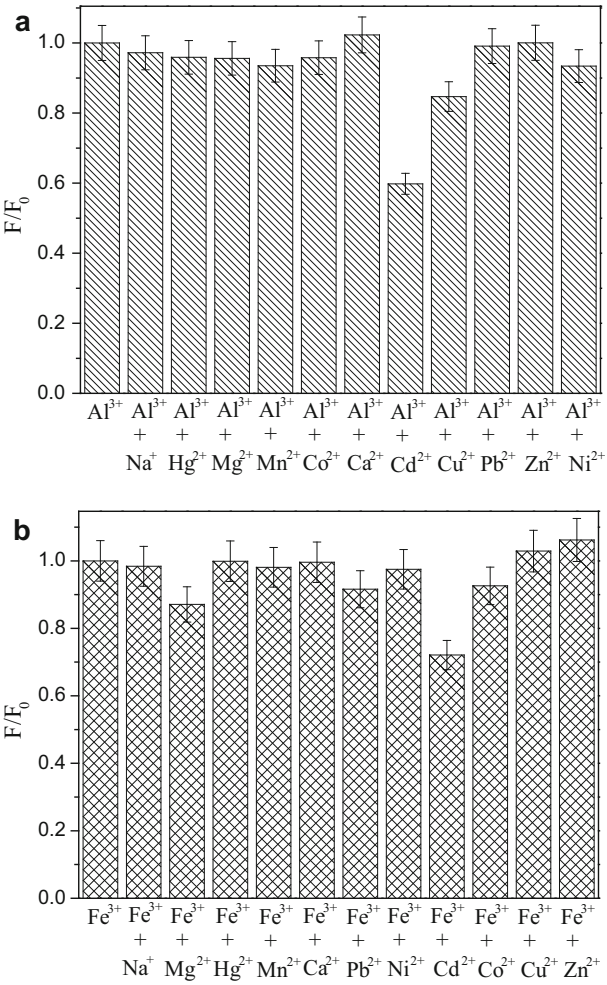

Fig. 4 Fluorescence responses of **1** (30 μmol/L) to Al^{3+} (30 μmol/L) **a** and Fe^{3+} (30 μmol/L) **b** in presence of other metal ions. F_0: fluorescence intensity of **1** containing Al^{3+} or Fe^{3+} without addition of competing ions, F: fluorescence intensity of **1** containing Al^{3+} or Fe^{3+} after addition of competing ions (300 μmol/L)

UV–Vis absorption responses of 1 to Al^{3+} or Fe^{3+}

The absorption spectral properties of **1** upon titration of Al^{3+} or Fe^{3+} were studied in THF/H_2O (9/1, v/v). As shown in Fig. 5a, the absorption spectrum of **1** displayed two absorption bands at 225 and 310 nm. Upon addition of Al^{3+}, the absorption intensity at 310 nm decreased, and at the same time a new absorption peak at 338 nm appeared and the absorbance increased with increasing concentration of Al^{3+}. The 28-nm redshift could be explained by the fact that coordination between **1** and Al^{3+} inhibited rotation of the σ-bond between the pyridine and benzothiazole

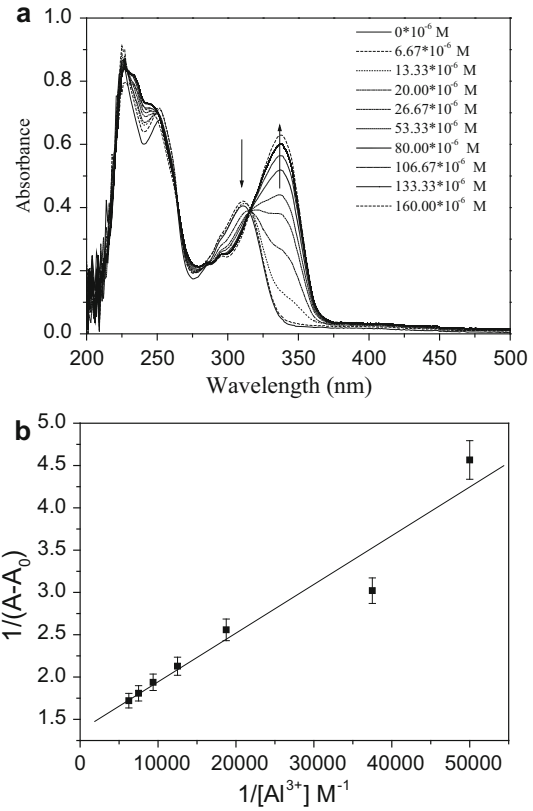

Fig. 5 **a** Absorption spectra of **1** (30 μmol/L) upon addition of Al^{3+} in THF/H_2O (9:1, v/v) and **b** Benesi–Hildebrand plot (absorbance at 338 nm) of **1** between $1/(A - A_0)$ and $1/[Al^{3+}]$

groups and increased the rigidity of the molecular skeleton. In addition, charge transfer between the electron-rich ligand and electron-deficient metal ions also increased the conjugation property of the molecule. The increase in the rigidity and the conjugation property of **1**-Al^{3+} turned on its fluorescence. A concomitant isosbestic absorption point at 315 nm indicated that only one intermediate complex was formed during the titration process. In view of the fluorescent Job's plot results, it could be concluded that only one 1:1 complex was formed in the **1**-Al^{3+} system.

The association constant of the complex **1**-Al^{3+} was calculated by the Benesi–Hildebrand expression (Eq. 1) [42].

$$\frac{1}{A - A_0} = \frac{1}{K_a(A_{max} - A_0)[Al^{3+}]} + \frac{1}{A_{max} - A_0}, \quad (1)$$

where A_0 is the absorbance of **1** at 338 nm in the absence of Al^{3+}, A is the absorbance of **1** at 338 nm at a certain concentration of Al^{3+}, A_{max} is the absorbance of **1** at a complete-interaction concentration of Al^{3+}, K_a is the association constant, and $[Al^{3+}]$ is the concentration of Al^{3+}. On the basis of the plot of $1/(A - A_0)$ versus $1/[Al^{3+}]$, the association constant was determined from the slope to be 2.99×10^4 M^{-1} (Fig. 5b).

The ratio between the absorbance at 338 nm and that at 310 nm of **1** increased linearly with increasing Al^{3+} concentration in the range of 6.67×10^{-6}–1.60×10^{-4} mol/L (Fig. 6). This result indicated that **1** showed high colorimetric selectivity to Al^{3+} and might be a promising colorimetric sensor for Al^{3+}.

A similar experimental result was obtained for the titration of Fe^{3+} (Fig. S5, ESM). Upon titration of Fe^{3+}, the new absorption peak and the concomitant isosbestic absorption point also appeared at 338 and 315 nm, respectively, indicating that only one intermediate complex was formed during the titration process. In view of the results of Job's plot, it could be concluded that only one 1:1 complex was formed during the titration of Fe^{3+} into the solution of **1**. The association constant of the complex between **1** and Fe^{3+} was also calculated by the Benesi–Hildebrand expression (Eq. 1) (as shown in Fig. S6, ESM) to be 6.86×10^3 M^{-1}. The ratio between the absorbance at 338 and 310 nm of **1** increased linearly with increasing Fe^{3+} concentration in the range of 0–1.60×10^{-4} mol/L (Fig. S7, ESM). This result indicated that **1** also showed high colorimetric selectivity to Fe^{3+} and might be a promising colorimetric sensor for Fe^{3+}.

The positions of the response wavelengths were the same for **1** toward Al^{3+} and Fe^{3+}. Under 365-nm lamp irradiation, the solutions of **1**-Al^{3+} and **1**-Fe^{3+} turned blue, while the solutions of **1** in the presence of other ions did not change at all (Fig. 7). It could still be found that the solution of **1** displayed a light-yellow color upon addition of Fe^{3+} because of the intrinsic color of Fe^{3+} (Fig. S8, ESM), and the solution of **1** exhibited no color upon addition of Al^{3+} as well as the other ions. Therefore, it is easy to distinguish the solution of Fe^{3+} from Al^{3+} in combination with the fluorescent spectra measurement. The paramagnetic nature of Fe^{3+} might quench the fluorescence of **1**-Fe^{3+} to some degree. The lower association constant of **1**-Fe^{3+} than that of **1**-Al^{3+} could also contribute to the superior Al^{3+} compared with Fe^{3+} sensitivity.

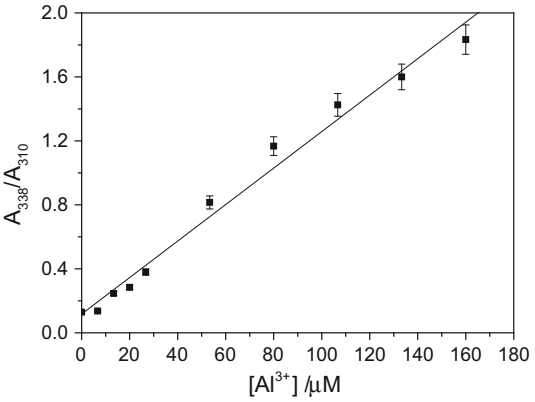

Fig. 6 Ratio between absorbance at 310 and at 338 nm of **1** upon titration of Al^{3+}

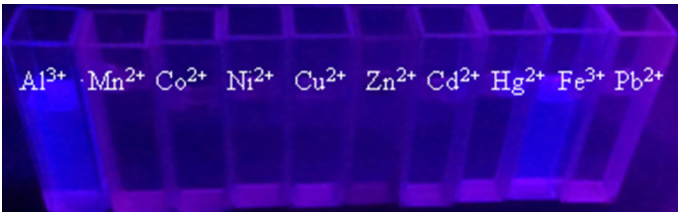

Fig. 7 Photograph of **1** (50 μmol/L) in THF/H_2O (v/v, 9:1) solution with 10 equiv metal ions under irradiation by 365-nm lamp

pH effect on fluorescence of 1 and 1-Al^{3+} complex

To determine a suitable pH range for **1** as a chemosensor for Al^{3+}, the fluorescence spectra of **1** with and without Al^{3+} in different pH solutions were investigated. As shown in Fig. 8, **1** revealed no fluorescence at 393 nm between pH 2.6 and 11.1. After addition of Al^{3+}, the fluorescence of **1**-Al^{3+} solution was far stronger than that of **1** with pH value less than 9. It is well known that Al^{3+} will precipitate as $Al(OH)_3$ in weak basic solution and change to AlO_2^- in strong basic solution. These results indicate that **1** can be applied for monitoring Al^{3+} fluorimetrically over a wide pH range.

Sensing mechanism

According to the absorption and emission properties of **1** with and without Al^{3+} or Fe^{3+}, the binding mechanism of **1** with Al^{3+} or Fe^{3+} was assumed. The fluorescence of the benzo[*d*]thiazole moiety was quenched by the intramolecular PET effect from the lone pair of electrons of the N atom on 2′ position of pyridine group to the adjacent benzo[*d*]thiazole. This PET effect would result in no fluorescence of **1**. After it was bound with Al^{3+} or Fe^{3+}, the lone pair of electrons on the nitrogen of **1** was stabilized, and intramolecular PET to the adjacent benzo[*d*]thiazole group upon

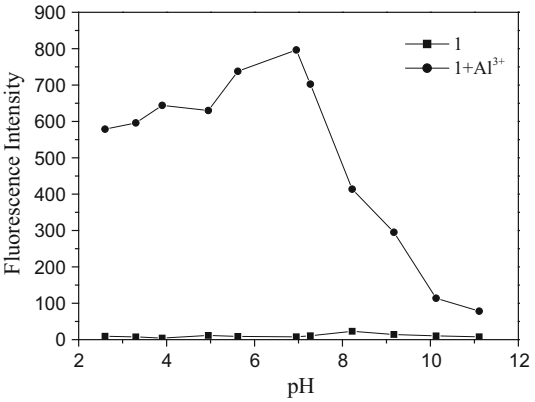

Fig. 8 Fluorescence intensities (393 nm) of **1** in THF/H_2O (30 μM) (9:1, v/v) with and without Al^{3+} (2 equiv) as a function of pH. **1**-Al^{3+} (*circle*) and **1** (*square*)

photoexcitation of **1** was thermodynamically unfavorable, resulting in the significant fluorescence enhancement (Scheme 2). Evidence was obtained by carrying out ESI mass analysis of **1**-Al^{3+}. **1** exhibited a peak at $m/z = 256.2$ (calcd. 256.3 for $C_{13}H_{12}N_4S$), which corresponded to $[\mathbf{1}]^+$ as shown in Fig. S3 (ESM). Several new peaks were clearly observed after $AlCl_3$ (60 μmol) was added to the solution of **1** (30 μmol), as shown in Fig. S9 (ESM), in which $m/z = 318.8$ corresponds to $[\mathbf{1} + Al + Cl]^+$ with chemical formula $C_{13}H_{12}AlClN_4S$ (calcd. 318.7) and $m/z = 301.2$ corresponds to $[\mathbf{1} + Al + H_2O]$ with formula $C_{13}H_{14}AlN_4OS$ (calcd. 301.1).

To further understand the recognition process of **1** toward Al^{3+}, highest occupied molecular orbital (HOMO) and lowest unoccupied molecular orbital (LUMO) distributions of **1** and $\mathbf{1} + Al^{3+}$ were determined by density functional theory (DFT) calculations, in which 6–31 g(d) basic set was used for C, H, N, S, and Cl, and lanl2dz was used for Al [43]. As shown in Fig. 9, the HOMO distribution of **1** was concentrated exclusively on the amino pyridine moieties without contribution from benzothiazole group. The LUMO distribution of **1** was concentrated on the benzothiazole group without contribution from pyridine group. The dihedral angle between pyridine and benzothiazole groups was about 88.2°. Although the HOMO distribution of $\mathbf{1} + Al^{3+}$ was still concentrated mainly on the amino pyridine moieties, the contribution of benzothiazole group and Al^{3+} was very obvious. The LUMO distribution of $\mathbf{1} + Al^{3+}$ was also mainly concentrated on the benzothiazole group, whereas the contribution of pyridine group and Al^{3+} was also very obvious. The dihedral angle between pyridine and benzothiazole groups changed to about 70.9°, indicating that the structural rigidity was promoted after **1** was bound with Al^{3+}. This effect made the excited state of $\mathbf{1} + Al^{3+}$ radiating. The calculation results were coincident with our experimental results.

Conclusions

A simple, sensitive "turn–on" chemosensor **1** for detection of Al^{3+} or Fe^{3+} was synthesized and characterized. The new sensor displayed ratiometric and colorimetric response toward Al^{3+} or Fe^{3+}. It exhibited fluorescence enhancement with good sensitivity in the presence of Al^{3+} or Fe^{3+} without significant interference from other metal ions such as Na^+, Hg^{2+}, Mg^{2+}, Mn^{2+}, Co^{2+}, Ca^{2+}, Cd^{2+}, Cu^{2+},

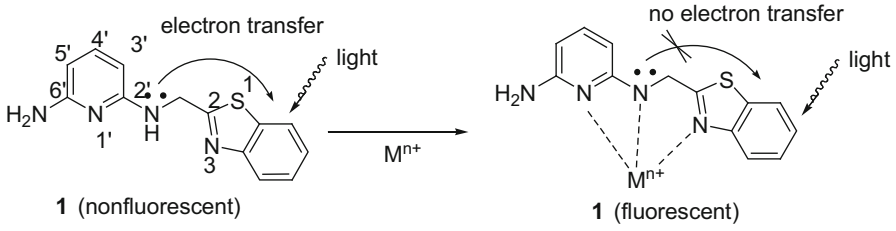

Scheme 2 Sensing mechanism of **1** towards metal ions

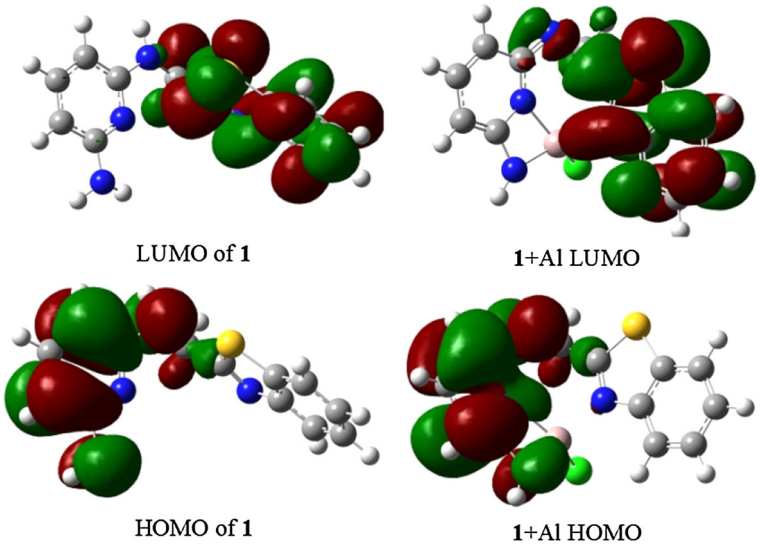

Fig. 9 Distributions of HOMO and LUMO of **1** and **1** + Al^{3+} determined by DFT calculations

Pb^{2+}, Zn^{2+}, and Ni^{2+}. The sensor could be applied for monitoring Al^{3+} or Fe^{3+} within a wide pH range. The coordination between **1** and Al^{3+} or Fe^{3+} increased the rigidity of the molecular skeleton and suppressed the PET process, resulting in fluorescence enhancement. The results indicated **1** to be a promising "turn-on" optical sensor for Al^{3+} or Fe^{3+}.

Acknowledgments This project was supported by the National Natural Science Foundation of China (NSFC) (21102037).

References

1. S.M.Z. Al-Kindy, Z. Al-Mafrigi, M.S. Shongwe, Luminescence **26**, 462–470 (2011)
2. E. Oliveira, H.M. Santos, J.L. Capelo, C. Lodeiro, Inorg. Chim. Acta **381**, 203–211 (2012)
3. K. Kaur, V.K. Bhardwaj, N. Kaur, N. Singh, Inorg. Chem. Commun. **18**, 79–82 (2012)
4. G. Papanikolaou, K. Pantopoulos, Toxicol. Appl. Pharmacol. **202**, 199–211 (2005)
5. W. Lin, L. Long, Y. Lin, Z. Cao, J. Feng, Anal. Chim. Acta **634**, 262–266 (2009)
6. Z. Liang, C. Wang, J. Yang, H. Gao, Y. Tian, X. Tao, M. Jiang, New J. Chem. **31**, 906–910 (2007)
7. V. Bhalla, N. Sharma, N. Kumar, M. Kumar, Sens. Actuators B Chem. **178**, 228–232 (2013)
8. F. Zhang, Y. Zhou, J. Yoon, Y. Kim, S. Kim, J. Kim, Org. Lett. **12**, 3852–3855 (2010)
9. J.S. Kim, D.T. Quang, Chem. Rev. **107**, 3780–3799 (2007)
10. D.T. Quang, J.S. Kim, Chem. Rev. **110**, 6280–6301 (2010)
11. J. Wu, W. Liu, J. Ge, H. Zhang, P. Wang, Chem. Soc. Rev. **40**, 3483–3495 (2011)
12. S. Ji, H. Guo, X. Yuan, X. Li, H. Ding, P. Gao, C. Zhao, W. Wu, W. Wu, J. Zhao, Org. Lett. **12**, 2876–2879 (2010)
13. Y. Chen, J. Zhao, H. Guo, L. Xie, J. Org. Chem. **77**, 2192–2206 (2012)
14. M. Yang, M. Sun, Z. Zhang, S. Wang, Talanta **105**, 34–39 (2013)
15. U. Fegade, S. Attarde, A. Kuwar, Chem. Phys. Lett. **584**, 165–171 (2013)
16. P. Cheng, K. Xu, W. Yao, E. Xie, J. Liu, J. Lumin. **143**, 583–586 (2013)
17. K. Sung, H.-K. Fu, S.-H. Hong, J. Fluoresc. **17**(4), 383–389 (2007)

18. S.E. Malkondu, Tetrahedron **70**(35), 5580–5584 (2014)
19. S. Goswami, S. Paul, A. Manna, RSC Adv. **3**, 25079–25085 (2013)
20. Y. Xu, D. Zhang, B. Li, Y. Zhang, S. Sun, Y. Pang, RSC Adv. **4**(23), 11634–11639 (2014)
21. M. Shellaiah, Y.-H. Wu, H.-C. Lin, Analyst **138**(10), 2931–2942 (2013)
22. S. Goswami, K. Aich, A.K. Das, A. Manna, S. Das, RSC Adv. **3**, 2412–2416 (2013)
23. D. Dey, J. Saha, A.D. Roy, D. Bhattacharjee, S.A. Hussain, Sens. Actuators B Chem. **195**, 382–388 (2014)
24. P. Xie, F. Guo, R. Xia, Y. Wang, D. Yao, G. Yang, L. Xie, J. Lumin. **145**, 849–854 (2014)
25. S. Goswami, A. Manna, S. Paul, A.K. Maity, P. Saha, C.K. Quah, H.-K. Fun, RSC Adv. **4**, 34572–34576 (2014)
26. J. Wang, Y. Li, N.G. Patel, G. Zhang, D. Zhou, Y. Pang, Chem. Commun. **50**, 12258–12261 (2014)
27. X. Fang, S. Zhang, G. Zhao, W. Zhang, J. Xu, A. Ren, C. Wu, W. Yang, Dyes Pigments **101**, 58–66 (2014)
28. X. Wan, T. Liu, H. Liu, L. Gu, Y. Yao, RSC Adv. **4**(56), 29479–29484 (2014)
29. S. Goswami, S. Paul, A. Manna, RSC Adv. **3**, 10639–10643 (2013)
30. S. Guha, S. Lohar, A. Sahana, A. Banerjee, D.A. Safin, M.G. Babashkina, M.P. Mitoraj, M. Bolte, Y. Garcia, S.K. Mukhopadhyay, D. Das, Dalton Trans. **42**(28), 10198–10207 (2013)
31. Q. Meng, H. Liu, C. Sen, C. Cao, J. Ren, Talanta **99**, 464–470 (2012)
32. S. Goswami, A. Manna, S. Paul, K. Aich, A.K. Das, S. Chakraborty, Dalton Trans. **42**, 8078–8085 (2013)
33. T. Ueno, T. Nagano, Nat. Methods **8**, 642–645 (2011)
34. Y. Ma, W. Luo, P.J. Quinn, Z. Liu, R.C. Hider, J. Med. Chem. **47**, 6349–6362 (2004)
35. B. Wang, J. Hai, Z. Liu, Q. Wang, Z. Yang, S. Sun, Angew. Chem. Int. Ed. **49**, 4576–4579 (2010)
36. X. Xie, Y. Qin, Sens. Actuators B Chem. **156**, 213–217 (2011)
37. D. Maity, T. Govindaraju, Chem. Commun. **46**, 4499–4501 (2010)
38. A. Banerjee, A. Sahana, S. Das, S. Lohar, S. Guha, B. Sarkar, S.K. Mukhopadhyay, A.K. Mukherjee, D. Das, Analyst **137**, 2166–2175 (2012)
39. H. Wang, J. Li, D. Yao, Q. Gao, F. Guo, P. Xie, Res. Chem. Intermed. **39**, 2723–2734 (2013)
40. P. Xie, F. Guo, D. Zhang, L. Zhang, Chin. J. Chem. **29**, 1975–1981 (2011)
41. A. Dondoni, G. Fantin, M. Fogagnolo, A. Medici, P. Pedrini, Tetrahedron **44**, 2021–2031 (1988)
42. H.A. Benesi, J.H. Hildebrand, J. Am. Chem. Soc. **71**, 2703–2707 (1949)
43. M.J. Frisch, G.W. Trucks, H.B. Schlegel, G.E. Scuseria, M.A. Robb, J.R. Cheeseman, J.A. Montgomery, T. Vrevenjr, K.N. Kudin, J.C. Burant, J.M. Millam, S.S. Iyengar, J. Tomasi, V. Barone, B. Mennucci, M. Cossi, G. Scalmani, N. Rega, G.A. Petersson, H. Nakatsuji, M. Hada, M. Ehara, K. Toyota, R. Fukuda, J. Hasegawa, M. Ishida, T. Nakajima, Y. Honda, O. Kitao, H. Nakai, M. Klene, X. Li, J.E. Knox, H.P. Hratchian, J.B. Cross, V. Bakken, C. Adamo, J. Jaramillo, R. Gomperts, R.E. Stratmann, O. Yazyev, A.J. Austin, R. Cammi, C. Pomelli, W.J. Ochterski, P.Y. Ayala, K. Morokuma, G.A. Voth, P. Salvador, J.J. Dannenberg, V.G. Zakrzewski, S. Dapprich, A.D. Daniels, M.C. Strain, O. Farkas, D.K. Malick, A.D. Rabuck, K. Raghavachari, J.B. Fores-man, J.V. Ortiz, Q. Cui, A.G. Baboul, S. Clifford, J. Cioslowski, B.B. Stefanov, G. Liu, A. Liashenko, P. Piskorz, I. Komaromi, R.L. Martin, D.J. Fox, T. Keith, M.A. Al-Laham, C.Y. Peng, A. Na-nayakkara, M. Challacombe, P.M.W. Gill, B. Johnson, W. Chen, M.W. Wong, C. Gonzalez, J.A. Pople, *Gaussian 03, revision B05* (Wallingford, Connecticut, 2003)